PHYSICAL REVIEW B **82**, 121201(R) (2010)

Electron spin coherence of phosphorus donors in silicon: Effect of environmental nuclei

Eisuke Abe,[1,2,*] Alexei M. Tyryshkin,[3] Shinichi Tojo,[2] John J. L. Morton,[1,4] Wayne M. Witzel,[5] Akira Fujimoto,[2] Joel W. Ager,[6] Eugene E. Haller,[6,7] Junichi Isoya,[8] Stephen A. Lyon,[3] Mike L. W. Thewalt,[9] and Kohei M. Itoh[2]

[1]*Department of Materials, Oxford University, Parks Road, Oxford OX1 3PH, United Kingdom*

[2]*School of Fundamental Science and Technology, Keio University, 3-14-1 Hiyoshi, 223-8522, Japan*

[3]*Department of Electrical Engineering, Princeton University, Princeton, New Jersey 08544, USA*

[4]*Clarendon Laboratory, Oxford University, Parks Road, Oxford OX1 3PU, United Kingdom*

[5]*Sandia National Laboratories, Albuquerque, New Mexico 87185, USA*

[6]*Lawrence Berkeley National Laboratory, 1 Cyclotron Road, Berkeley, California 94720, USA*

[7]*Department of Materials Science and Engineering, University of California, Berkeley, California 94720, USA*

[8]*Graduate School of Library, Information and Media Studies, University of Tsukuba, 1-2 Kasuga, 305-8550, Japan*

[9]*Department of Physics, Simon Fraser University, Burnaby, British Columbia, Canada V5A 1S6*

(Received 10 July 2010; revised manuscript received 8 August 2010; published 2 September 2010)

We report electron paramagnetic resonance (EPR) experiments of phosphorus donors in isotopically controlled silicon single crystals. By varying the concentration of the ^{29}Si isotope, f, from 0.075% to 99.2%, we systematically study the effect of the environmental nuclear spins on the donor-electron spin. We find excellent agreement between experiment and theory for decoherence times due to nuclear-induced spectral diffusion, clarifying that the nuclear-induced decoherence is dominant in the range of f studied. We also observe that the EPR linewidth shows a transition from the square-root dependence to the linear dependence on f, in agreement with theoretical predictions.

DOI: 10.1103/PhysRevB.82.121201 PACS number(s): 76.30.−v, 76.60.Lz, 03.67.Lx, 28.60.+s

Recent prospects for scalable solid-state quantum information processors have generated a considerable interest in electron-spin coherence of phosphorus donors in silicon.[1,2] Although electron paramagnetic resonance (EPR) in Si:P is now a textbook example of how an electron spin in a solid interacts with nuclei, its coherence properties were largely unexplored until recently. The donor-electron spin is hyperfine-coupled to the ^{31}P nucleus with $I=1/2$, exhibiting a doublet separated by 42 G in the EPR spectrum. In addition, host ^{29}Si nuclei with $I=1/2$, randomly occupying 4.7% of the lattice sites of natural Si, are mutually coupled through the magnetic dipolar interactions. By flip flopping their spins, the environmental nuclei cause a temporal change in the electron-spin precession frequency. This process, termed as nuclear-induced spectral diffusion, is regarded as a major source of decoherence in Si:P as well as in many other quantum computing schemes based on electron spins. Recent experimental studies include measurements of electron-spin coherence in natural, and ^{28}Si- and ^{29}Si-enriched samples,[3–6] and demonstration of the storage and retrieval of electron-spin coherence into and from the ^{31}P nuclear spin.[7] Research has also been further extended to other donors such as bismuth.[8]

In this Rapid Communication, building on our previous works,[3,5,6] we study electron-spin decoherence due to environmental nuclear spins in isotopically controlled Si:P single crystals in which the ^{29}Si concentration f ranges from 0.075% to 99.2%. Our experimental observations are in excellent agreement with nonstochastic and microscopic theory called a quantum cluster expansion method. The details of the theory developed by Witzel *et al.* can be found in Refs. 9–11. We also present the measurements of the EPR linewidth as a function of f, which is well accounted for by theoretical calculations. The tunability of the ^{29}Si concentration and long intrinsic decoherence times of the P donor make Si:P an important testbed for proposed theories for spectral diffusion-induced electron-spin decoherence. Such models can then be applied to other materials systems, including III-V materials based on Ga, As, and Al (all of which carry nonzero nuclear spins) or other group IV hosts such as C and Ge. An example of the latter is the study of nitrogen-vacancy centers in diamond as a function of host ^{13}C concentration.[12,13]

Isotopically controlled Si is now in wide use for the studies of optical and thermal properties of Si, as well as for precise determination of the Avogadro constant.[14,15] High-quality single crystals have been grown by either a Czochralski (Cz) or floating zone (Fz) method. For this work, we prepared six samples, namely, ^{29}Si-0.08% ($f=0.00075$, $N_d=1.2\times10^{15}$ cm^{-3}, Fz grown), ^{29}Si-1% ($f=0.012$, $N_d=0.7\times10^{15}$ cm^{-3}, Fz), ^{29}Si-5% ($f=0.047$, $N_d=0.8\times10^{15}$ cm^{-3}, Cz), ^{29}Si-10% ($f=0.103$, $N_d=1.6\times10^{15}$ cm^{-3}, Fz), ^{29}Si-50% ($f=0.479$, $N_d=0.6\times10^{15}$ cm^{-3}, Fz), and ^{29}Si-100% ($f=0.992$, $N_d=0.8\times10^{15}$ cm^{-3}, Cz), where f was determined from secondary ion mass spectroscopy (SIMS) and the net donor concentration N_d was determined from Hall measurements. N_d is fixed to about 10^{15} cm^{-3} throughout the samples. This value has been chosen to minimize unwanted dipolar interactions among the donor-electron spins while still ensuring good measurement sensitivity. Pulsed EPR experiments were carried out using X-band spectrometers (Bruker) equipped with helium-flow cryostats (Oxford Instruments). The static magnetic field B_0 was applied in the $(1\bar{1}0)$ plane and the angle with respect to the [001] crystal axis is defined as shown in Fig. 1(a). In the following, B_0 was fixed at the center of the high-field line of the Si:P doublet. We employed a two-pulse electron spin echo (ESE) sequence $[\theta_1]$-τ-$[\theta_2]$-τ-echo [Fig. 1(b)], where

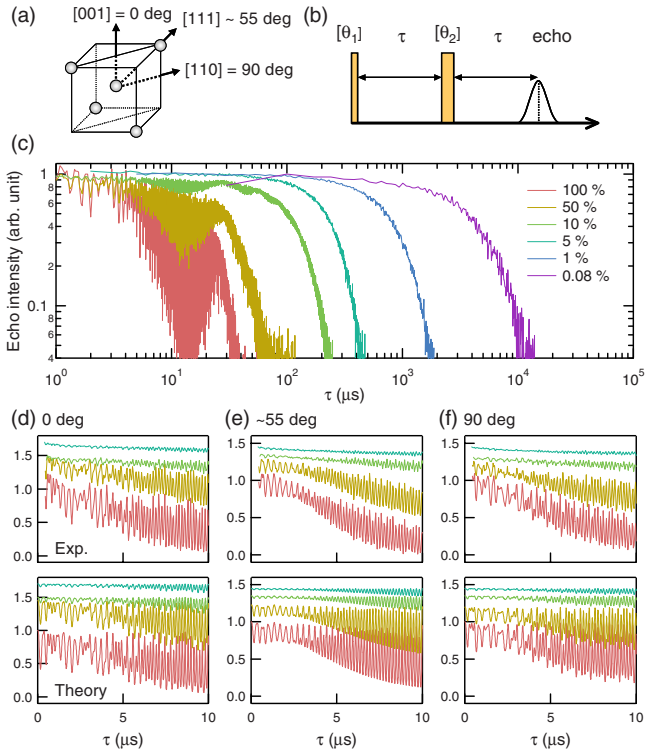

FIG. 1. (Color online) (a) Definition of angles. The static magnetic field B_0 was applied parallel to the $(1\bar{1}0)$ plane of silicon crystals. By rotating samples about the $[1\bar{1}0]$ axis, the direction of B_0 is varied from [001] (0°) to [110] (90°). (b) Two-pulse ESE sequence. The tipping angles θ_1 and θ_2 are 90° and 180° except for the case of ^{29}Si-0.08%. See the text. (c) Log-log plot of ESE decay curves at 0°. The data are for ^{29}Si-0.08%, 1%, 5%, 10%, 50%, and 100% from right to left (slow-to-fast decays). [(d)–(f)] Experimental (top panels) and theoretical (bottom panels) ESEEM at early time for ^{29}Si-5%, 10%, 50%, and 100% (from top to bottom) at three representative angles. The traces are offset for clarity.

$\theta_{1(2)}$ is the tipping angle of the first (second) pulse and τ is the interpulse delay. Except for ^{29}Si-0.08%, θ_1 and θ_2 were 90° and 180°, respectively. In ^{29}Si-0.08%, we used $\theta_1=90°$ and $\theta_2=70°$ in order to minimize the effect of instantaneous diffusion (decoherence caused by flips of dipole-coupled electron spins as driven by the applied microwave pulses).[3,6]

In a study of nuclear-induced spectral diffusion in Si:P, the measurement temperature T must be low enough to ensure the spin-lattice relaxation time T_1 (arising from an Orbach process[16]) is long enough to give no appreciable contribution to the measured T_2. For ^{29}Si-0.08%, 50%, and 100%, T was 7–8 K and the ESE sequence was repeated at time intervals much longer than T_1. For ^{29}Si-1%, T was 5 K and a light-emitting diode (1070 nm) was illuminated for short time (50 ms) after each ESE sequence in order to shorten the otherwise extremely long T_1. For ^{29}Si-5% and 10%, both methods were tested, and confirmed to give nearly identical results. In all cases, the observed time scales for phase relaxation are much shorter than the corresponding T_1 in the dark, and in our discussions below we can assume that T_1 processes are of no importance.

Figure 1(c) shows a log-log plot of ESE decay curves at 0° ($B_0\|[001]$). It is clearly observed that the lower-f samples show better coherence properties. The strong oscillations observed in the high-f samples are ESE envelope modulation (ESEEM). As analyzed previously,[5,11] this oscillation pattern is caused by the quantum-mechanical interference between the donor-electron spin and ^{29}Si nuclei adjacent to the P atom. The behaviors at early time, both experimental and theoretical,[11] are shown in Figs. 1(d)–1(f). Theory reproduces fine details of the modulation patterns for the respective angles as well as the dependence of the modulation amplitudes on f. Experimentally, even a slight misalignment of the crystal axis can result in a large change in the modulation amplitudes, which is a possible reason for the difference in the amplitudes between experiment and theory.

Next we examine the nuclear-induced spectral diffusion time T_{SD}. We note that nuclei participating in ESEEM are not the same as those causing spectral diffusion. The former nuclei, residing in close vicinity to the donor and experiencing large hyperfine fields, cannot flip flop their spins due to energy conservation. The latter consists of a much larger group of nuclei that are far away from the donor; these nuclei only see very weak hyperfine fields, and the flip flop is allowed. Thus we may regard ESEEM and nuclear-induced spectral diffusion as independent. Figure 2 presents the full details of the two-pulse ESE decay curves. It is apparent that the ESE decay envelopes are not single exponential. To extract T_{SD}, we fit those envelopes to the form

$$V(\tau) = V_0(\tau)\exp[-(2\tau/T_{SD})^n - (2\tau/T_2)]. \quad (1)$$

Here, the spectral diffusion decay is assumed to take a stretched-exponential decay with $n>1$.[6] A single-exponential decay term is included to account for other decoherence mechanisms and T_2 is assumed to be independent of the direction of B_0. The values of the parameters T_{SD} and n, obtained from fits to Eq. (1), are plotted in Fig. 3. As already evident from Fig. 2, T_{SD} reaches its maximum at 0° ($B_0\|[001]$) and its minimum at around 55° ($B_0\|[111]$), reflecting the anisotropy of the nuclear dipolar interaction. We can directly compare experimental values of T_{SD} with those obtained from theory. The dotted and dashed curves in Fig. 3(b) are simulations using the cluster method,[9,10] showing an excellent agreement for extreme orientations of 0° and 55° in $f>1\%$. Although at $f=0.08\%$ the theory is still in a reasonable quantitative agreement with experiment, there is a clear qualitative difference in that the experiment still shows a clear anisotropy in T_{SD} while theory predicts no such anisotropy. In principle, with decreasing f the probability of finding next-neighboring ^{29}Si-^{29}Si nuclear pairs in a close proximity to a donor also decreases and so the angular dependence in T_{SD} should eventually vanish. However, our model apparently predicts this transition takes place at a higher f than that observed in experiment, and the reason for this discrepancy is as yet unclear. We have considered several possible explanations, such as nuclear flip flops involving more than two nuclei (larger clusters), which are not accounted in our simulations, or hyperfine-mediated nuclear flip flops but currently have not reached a satisfactory answer.

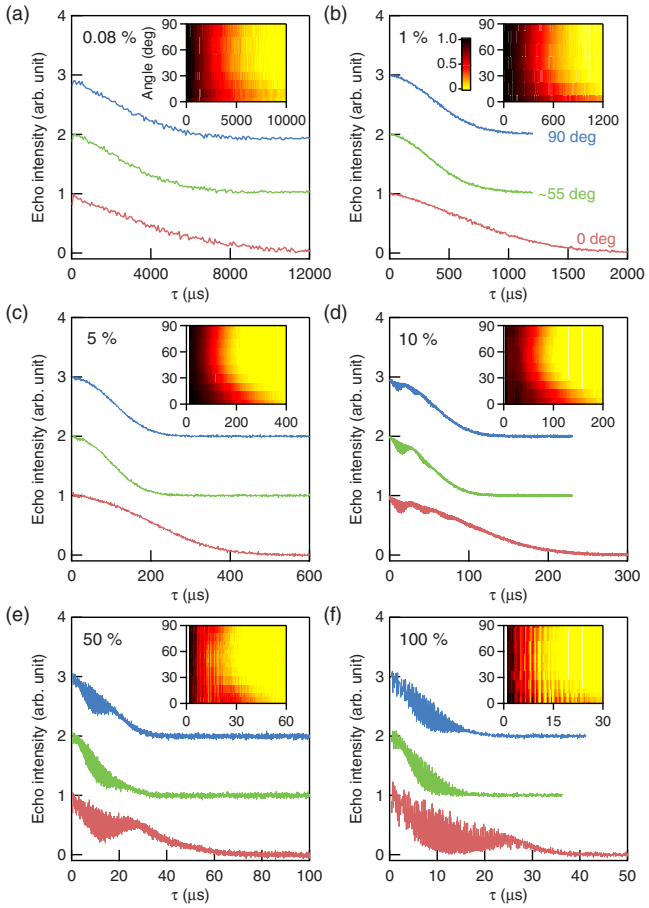

FIG. 2. (Color online) Two-pulse ESE decay curves for the three representative angles. The base lines are offset for clarity. Note the different time scales in different samples. The insets are color plots showing the full angular dependence of the echo decay curves.

A few remarks are worth mentioning at this point. In the fitting, we always found T_2 to be much longer than T_{SD}. This certifies *a posteriori* that the major decoherence mechanism in our experimental conditions is the nuclear-induced spectral diffusion. In addition, we did not include T_2 as a parameter for ^{29}Si-50% and 100% since the fitting errors are fairly large due to the presence of ESEEM. The errors in n are also large (but still between 2 and 2.5), and n for these samples are not plotted in Fig. 3(b). On the other hand, the errors in T_{SD} are small, as in this case T_{SD} is always close to the time at which the echo envelope decays to $1/e$ of the initial intensity. Second, in measuring ^{29}Si-1% and 0.08%, special care was taken to circumvent the effect of phase fluctuations of the quadrature-detected echo signals. As reported previously,[3,6] this occurs at τ longer than about 500 μs in our apparatus. The most effective and most straightforward way to counter this problem was to measure the signal in single shots.

Finally, we turn our attention to the linewidth of the Si:P EPR spectra. As the orbital part of the electron wave function spreads over thousands of lattice sites, the electron is subject to the hyperfine fields of the ^{29}Si nuclei within its extent. The ^{29}Si nucleus at the lth site shifts the resonant frequency of the electron spin by $\pm a_l/2$, depending on direction of

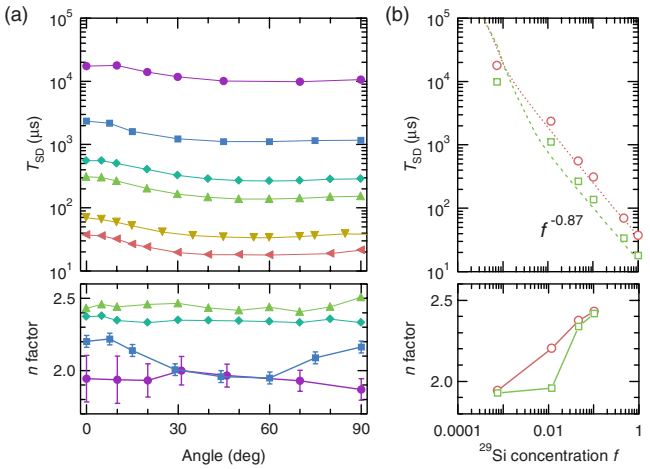

FIG. 3. (Color online) (a) Angular dependence of spectral diffusion time T_{SD} and stretched exponent n for ^{29}Si-0.08% (circle), 1% (square), 5% (diamond), 10% (triangle), 50% (down triangle), and 100% (left triangle). The fitting errors are within the sizes of the respective symbols, unless given explicitly. (b) ^{29}Si concentration dependence of T_{SD} and n at 0° (circle) and 55° (square). For $f>1\%$, theory predicts the $f^{-0.87}$ power law, in agreement with experiment. n falls on between 1.8 and 2.6, consistent with a theoretical prediction of about 2.3.

nuclear spin, where a_l is the isotropic hyperfine field at the lth site. Consequently, random static shifts of the individual electron-spin resonant frequencies lead to inhomogeneous broadening of the EPR lines.

Two different regimes have been identified for the dependence of the EPR linewidth on f.[17,18] In the high-f regime ($f>10\%$), the inhomogeneous broadening is describable by a Gaussian line shape with a full width at half maximum (FWHM) linewidth of $\Delta B_G = 2\sqrt{2\ln 2}\times\sqrt{f\Sigma_l(a_l/2)^2}$.[17] In the low-$f$ regime, however, the line shape resembles Lorentzian, rather than Gaussian, with the linewidth ΔB_L given as $\pi f\sqrt{(\Sigma_l a_l^2)^3/12\Sigma_l a_l^4}$. The latter expression while not explicitly derived here, follows straightforwardly from other equations by Kittel and Abrahams.[18] We demonstrate below that these two expressions accurately describe the donor EPR linewidth in high- and low-f regimes, respectively, with the crossover occurring around the natural abundance of ^{29}Si.

Figure 4(a) shows the high-field lines of the donor doublet using continuous-wave (cw) EPR and Fig. 4(b) plots the FWHM of these lines as a function of f. In each case, the same line shapes are observed using pulsed EPR, where the intensity of the ESE signal is measured as a function of B_0 with τ fixed. For $f\geq 4.7\%$, the lines are Gaussian [see Fig. 4(c)], and therefore the first expression for ΔB_G should be appropriate. The sums such as $\Sigma_l a_l^2$ and $\Sigma_l a_l^4$ are readily computed using reported values of a_l for 176 lattice sites determined by electron-nuclear double resonance.[20,21] The calculated value of $2\sqrt{2\ln 2}\times\sqrt{\Sigma_l(a_l/2)^2}$ is 11.6 G, which accounts for the majority of the experimental width for $f=99.2\%$, 12.2 G. The rest of thousands of sites will have very small isotropic hyperfine constants, and make no substantial contribution to the linewidth. The dashed line in Fig. 4(b) shows $\Delta B_G = 11.6\ \text{G}\times f^{0.5}$, which agrees well with the experimental points for $f\geq 4.7\%$, as expected. For $f\leq 1.2\%$,

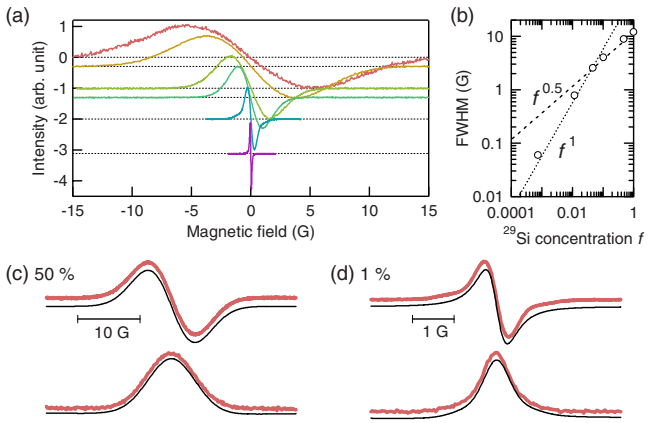

FIG. 4. (Color online) (a) cw EPR spectra. Only the high-field lines of the doublet peaks are shown. The horizontal axis is given as the offset from the resonance field. The base lines are offset for clarity (from top to bottom, ^{29}Si-100%, 50%, 10%, 5%, 1%, and 0.08%) and are determined as $\log_{10} f$ [e.g., the baseline for ^{29}Si-10% is $\log_{10}(0.1)=-1$]. (b) ^{29}Si concentration dependence of the FWHM of the spectra [see also Ref. 19]. (c) (Top) The thick gray (red online) line shows the cw spectrum of ^{29}Si-50%. The thin black line is fit by the first derivative of Gaussian. (Bottom) The thick gray (red online) line shows the field-sweep pulsed spectrum and the thin black line is the integral of the cw spectrum. The lines are offset for clarity. (d) Similar data for ^{29}Si-1%. The spectrum resembles Lorentzian. The thin black line in the top panel is fit by the first derivative of Lorentzian.

the line shapes resemble Lorentzian [see Fig. 4(d)] and a deviation from the $f^{0.5}$ power law is observed. Using the second expression, we obtain $\Delta B_L=57.6\ \mathrm{G}\times f$, which is drawn as the dotted line in Fig. 4(b). This explains the behavior for $f\leq 1.2\%$ quite well, and we observe a clear transition from the square-root dependence to the linear dependence on f, with the crossover occurring around the natural abundance.

In summary, we have provided a description of the role of the environmental nuclear spins on the P donor-electron spins in Si. Experimental T_{SD}, the behavior of ESEEM, and the EPR linewidth are well explained by theory. The only discrepancy between experiment and theory has been found in the lowest f sample, where the anisotropy in T_{SD} still survives while theory predicts disappearance of the anisotropy in this regime. In the future, further isotope purification will clarify this issue, as well as the point where another decoherence source, such as a dipolar interaction between donors, supersedes the nuclear-induced decoherence.

We thank H.-J. Pohl for the purified ^{29}Si source and A. Takano for SIMS measurements of several samples. J.J.L.M. was supported by the Royal Society. Work at Princeton was supported by the NSF through the Princeton MRSEC under Grant No. DMR-0213706 and by the NAS/LPS through LBNL under Grant No. MOD 713106A. Work at Keio was supported in part by the Grant-in-Aid for Scientific Research by MEXT, in part by Special Coordination Funds for Promoting Science and Technology, in part by JST-EPSRC Strategic International Cooperative Program, in part by the Funding Program for Science and Technology FIRST, and in part by the Global Center of Excellence at Keio University. Sandia National Laboratories is a multiprogram laboratory operated by Sandia Corporation, a wholly owned subsidiary of Lockheed Martin company, for the U.S. Department of Energy's National Nuclear Security Administration under Contract No. DE-AC04-94AL85000. Work at Lawrence Berkeley National Laboratory was supported by the Director, Office of Science, Office of Basic Energy Sciences, Materials Sciences and Engineering Division of the U.S. Department of Energy under Contract No. DE-AC02-05CH11231.

*eisuke.abe@materials.ox.ac.uk

[1] B. E. Kane, Nature (London) **393**, 133 (1998).
[2] R. Vrijen, E. Yablonovitch, K. Wang, H. W. Jiang, A. Balandin, V. Roychowdhury, T. Mor, and D. DiVincenzo, Phys. Rev. A **62**, 012306 (2000).
[3] A. M. Tyryshkin, S. A. Lyon, A. V. Astashkin, and A. M. Raitsimring, Phys. Rev. B **68**, 193207 (2003).
[4] E. Yablonovitch, H. W. Jiang, H. Kosaka, H. D. Robinson, D. S. Rao, and T. Szkopek, Proc. IEEE **91**, 761 (2003).
[5] E. Abe, K. M. Itoh, J. Isoya, and S. Yamasaki, Phys. Rev. B **70**, 033204 (2004).
[6] A. M. Tyryshkin, J. J. L. Morton, S. C. Benjamin, A. Ardavan, G. A. D. Briggs, J. W. Ager, and S. A. Lyon, J. Phys.: Condens. Matter **18**, S783 (2006).
[7] J. J. L. Morton, A. M. Tyryshkin, R. M. Brown, S. Shankar, B. W. Lovett, A. Ardavan, T. Schenkel, E. E. Haller, J. W. Ager, and S. A. Lyon, Nature (London) **455**, 1085 (2008).
[8] R. E. George, W. Witzel, H. Riemann, N. V. Abrosimov, N. Nötzel, M. L. W. Thewalt, and J. J. L. Morton, Phys. Rev. Lett. **105**, 067601 (2010).
[9] W. M. Witzel, R. de Sousa, and S. Das Sarma, Phys. Rev. B **72**, 161306 (2005).
[10] W. M. Witzel and S. Das Sarma, Phys. Rev. B **74**, 035322 (2006).
[11] W. M. Witzel, X. Hu, and S. Das Sarma, Phys. Rev. B **76**, 035212 (2007).
[12] N. Mizuochi *et al.*, Phys. Rev. B **80**, 041201 (2009).
[13] J. R. Maze, J. M. Taylor, and M. D. Lukin, Phys. Rev. B **78**, 094303 (2008).
[14] M. Cardona and M. L. W. Thewalt, Rev. Mod. Phys. **77**, 1173 (2005).
[15] P. Becker, H. Bettin, P. De Bièvre, C. Holm, U. Kütgens, F. Spieweck, J. Stümpel, S. Valkiers, and W. Zulehner, IEEE Trans. Instrum. Meas. **44**, 522 (1995).
[16] T. G. Castner, Jr., Phys. Rev. Lett. **8**, 13 (1962).
[17] W. Kohn, *Solid State Physics* (Academic Press, New York, 1957), Vol. 5, p. 257.
[18] C. Kittel and E. Abrahams, Phys. Rev. **90**, 238 (1953).
[19] In ^{29}Si-0.08%, the observed linewidth of 90 mG was limited by the inhomogeneity in B_0 and by detection spectral bandwidth. Plotted in the figure is 60 mG, which is obtained after correcting the two instrumental effects.
[20] G. Feher, Phys. Rev. **114**, 1219 (1959).
[21] E. B. Hale and R. L. Mieher, Phys. Rev. **184**, 739 (1969).